Available online at www.sciencedirect.com

SciVerse ScienceDirect

Energy Procedia 00 (2013) 000–000

Energy Procedia

www.elsevier.com/locate/procedia

GHGT-11

The effect of geological structure and heterogeneity on CO_2 storage in simple 4-way dip structures; a modeling study from the UK Southern North Sea

J.D.O. Williams[a,*], M. Bentham[a], M. Jin[b], G. Pickup[b], E. Mackay[b], D. Gammer[c], A. Green[c]

[a]*British Geological Survey, Kinsgley Dunham Centre, Keyworth, NG12 5GG, UK*
[b]*Institute of Petroleum Engineering, Heriot-Watt University, Riccarton Campus, Edinburgh, EH14 4AS, UK*
[c]*The Energy Technologies Institute, Holywell Building, Holywell Way, Loughborough, LE11 3UZ, UK*

Abstract

The Bunter Sandstone Formation in the Southern North Sea is folded into a number of simple 4-way dip-closed structures (domes). Most of these structures are saline water-bearing, although some of them do contain significant gas accumulations, suggesting that the brine-saturated domes may have potential for the long-term storage of CO_2. This study investigates the effect of geological structure and heterogeneity on CO_2 storage through the use of geological models and reservoir simulation. Dynamic modeling focussed on the determination of the storage efficiency of a particular dome and from this, its CO_2 storage capacity. Under initial modeling conditions, a storage efficiency of around 19 % was derived, though this is shown to be highly sensitive to a range of uncertain parameters. An interesting interplay exists between the reservoir heterogeneity and dome structure, whereby the evolving CO_2 plume is prevented from rising buoyantly to the top of the formation by the presence of impermeable horizons, which facilitates rapid migration towards the structural spill-points. Sensitivity analysis further emphasizes the importance of characterizing reservoir heterogeneity in studies for long-term carbon capture and storage.

Selection and/or peer-review under responsibility of GHGT

Keywords: Bunter Sandstone; Reservoir simulation; Heterogeneity; CO_2 storage efficiency

* Corresponding author. Tel.: +44(0)115 936 3100; fax: +44(0)115 936 3200.
E-mail address: jdow@bgs.ac.uk.

1. Introduction

The saline aquifer portions of the Bunter Sandstone Formation are considered likely to have significant potential for the geological storage of CO_2 in the UK sector of the Southern North Sea [1]. Factors contributing to its suitability as a reservoir for CO_2 include the following:

- It has a large areal extent, and is in close proximity to onshore emission sources.
- It is commonly 200–350 m thick.
- Much of the offshore extent lies at sufficient burial depths for CO_2 storage.
- Reservoir properties are considered to be fair to good.

In addition to these factors, the Bunter Sandstone contains numerous 4-way dip-closed structures (henceforth referred to as Bunter domes) formed by post-depositional halokinesis in underlying halite-dominated strata of the Zechstein Group. Where unaffected by faulting, the domes form structural traps that could be utilized to store significant quantities of injected CO_2. The Bunter Sandstone is overlain over much of the UK Southern North Sea by mudstones of the Haisborough Group, which form an effective seal in several Bunter Sandstone-reservoir gas fields. Over much of the area, this seal is enhanced by the presence of up to three halite members within the Haisborough Group. The non-gas-bearing domes are saturated with highly saline brine (around 180,000 parts per million). Three of these domes are evaluated here for the long-term storage of supercritical CO_2, through geological modeling and reservoir simulation.

2. Methodology

The aims of this study were to characterize part of the Bunter Sandstone containing a number of brine-saturated domes through detailed geological modeling, and to simulate the injection of industrial quantities of CO_2 into the formation in order to examine the likely range of storage efficiencies that could be achieved. Here, the storage efficiency is defined as the total volume of stored CO_2, divided by the pore volume of the dome, or of the multiple domes within which it is stored. The study also addressed the important issues of CO_2 migration and containment within the defined storage complex, along with the effects of pore-fluid pressure rise resulting from CO_2 injection. In addition, the sensitivity of injection to a range of boundary conditions and other uncertain parameters were examined. The following workflow was used:

- Selection of region for detailed modeling.
- Structural/geocellular modeling.
- Reservoir characterization and petrophysical modeling.
- Base-case reservoir simulation to calculate the storage efficiency of a single dome (E_d).
- Sensitivity analysis and examination of uncertain parameters affecting storage efficiency, including aquifer size, heterogeneity, and pressure interference caused by injection into multiple structures.

2.1. Selection of region for detailed modeling

A volume of the Bunter Sandstone containing three domes was selected for detailed modeling (Figure 1). One particular dome (Dome A) was selected as the primary focus for study, and was used in the base-case simulation for the following reasons:

- It falls near the middle of the size range for the Bunter domes.
- It has a considerable degree of structural closure (544 m from crest to spill-point).
- It is not affected by significant faulting.
- The crest of the structure lies at an appropriate depth for CO_2 storage (approximately 1186 m sub-sea).

The selected area is thought to be located within a much larger connected portion of the Bunter Sandstone saline aquifer with a volume of about 280 km^3, which at its limits may be closed by significant fault zones and salt walls. This is comparable to the area considered by [2] and [3], and while this additional connected aquifer volume is not explicitly represented in the model, it is accounted for using numerical aquifer volumes. Aquifer size and volume is regarded as a significant uncertainty, and is therefore addressed during the sensitivity analysis.

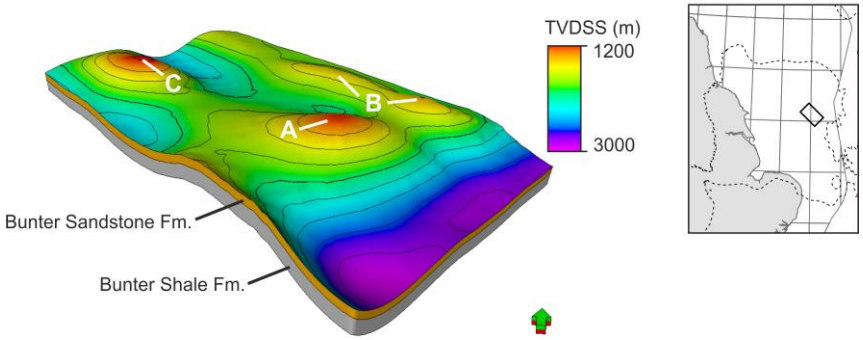

Fig. 1. Perspective view of the Bunter Sandstone model. Individual domes are labeled. While the underburden is shown (Bunter Shale Formation), the Haisborough Group caprocks are hidden for clarity. Model dimensions are approximately 25 x 44 km. Location of the model area and extent of the Bunter Sandstone are shown on the inset map.

2.2. Structural modeling

Most of the modeled area and the entirety of Dome A are well imaged by 3D seismic reflection data (PGS MegaMerge). Within the model area, no faults have been identified with a throw that significantly juxtaposes the Bunter Sandstone against the caprocks, and therefore no faults are believed to pose a significant risk to containment due to the high clay content of the immediately overlying Haisborough Group. For this reason, faults were not included in the geocellular model. Depth converted surfaces derived from seismic interpretation were available for the top Bunter Sandstone Formation and top Haisborough Group, and these were validated against existing well data supplied by IHS. Additional stratigraphic zonation was achieved using isopach maps derived from the well data. These surfaces form the basis of the geocellular model. The structure of the Bunter Sandstone in the model area is shown in Figure 1.

In addition, five intra-reservoir zones were identified within the Bunter Sandstone, and correlated throughout the model area using wireline geophysical logs. Each of the reservoir zones were layered appropriately, depending on the degree of intra-zone variations observed from the geophysical logs.

3. Reservoir characterization

The Bunter Sandstone was deposited in an arid to semi-arid fluvial environment, which to the north of the model area consists of alluvial fans dissected by braided fluvial channels [4]. Sediment was derived from the west–southwest, draining towards a playa lake to the north and northeast, transecting a low relief braidplain [5]. Sheetflood complexes are abundant, while individual channels are believed to exhibit a low degree of sinuosity [6]. The porosity and permeability of the reservoir is thus influenced by rapid variations in lithology, and by variable degrees of cementation which has locally occluded the porosity, resulting in reservoir property distributions that are difficult to predict. Some cemented layers can be identified from the geophysical logs, as they generally exhibit a low gamma ray response in addition to a reduction in sonic velocity and sharp increase in density. Figure 2a shows the typical geophysical log response associated with the Bunter Sandstone Formation in the model area, and indicates the interpreted depositional environment of each reservoir zone. Of particular note is a cemented sandstone layer at the top of Zone 4, roughly half way up through the reservoir which divides the reservoir into two distinct zones (Figure 2a). This can be correlated across all but two of the wells within the model area, and is prevalent over a distance of at least 20 km from the model area towards the northeast. However, whether it is truly laterally continuous is uncertain.

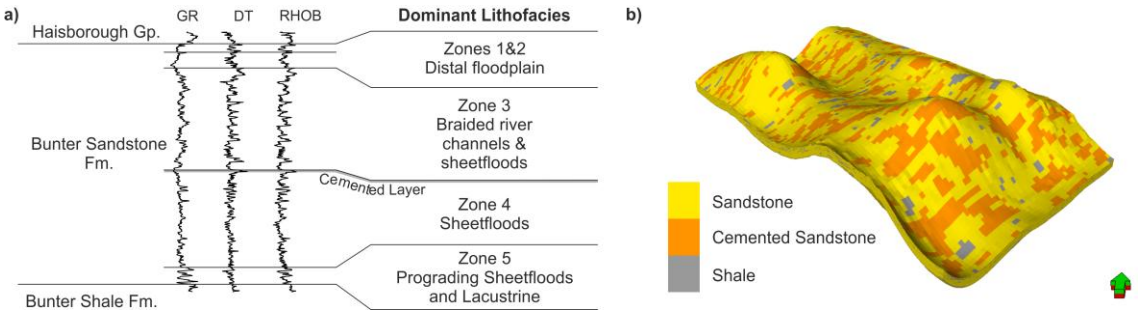

Fig. 2. a) Typical geophysical log response of the Bunter Sandstone in the model area, and interpreted depositional environments of the reservoir subdivisions. Note the presence of a thin cemented sandstone layer at the top of Zone 4. b) Perspective view showing distribution of lithofacies. Note the abundance of patchy cemented sandstone at the top of the reservoir, where cementation has preferentially affected higher permeability sandstones.

3.1. Distribution of lithofacies

Petrophysical analysis was used to divide the reservoir into three categories of lithofacies; non-cemented sandstone, cemented sandstone with occluded porosity, and shale. Upscaled lithofacies were distributed throughout the reservoir in accordance with the conceptual depositional environment for each reservoir zone (Figure 2b). This was achieved through a combination of log correlation and stochastic modeling techniques, including object-based modeling and Truncated Gaussian Simulation. The distributions in each zone honor those observed from the logs, and include vertical and lateral trends interpreted from the well data.

3.2. Petrophysical modeling

Porosity logs were calculated for the non-cemented sandstone using geophysical logs, and upscaled to the 3D grid. In order to represent local heterogeneities, Sequential Gaussian Simulation (SGS) was used to generate a stochastic distribution of porosity throughout the non-cemented sandstones, honoring the data ranges and trends observed from the porosity logs. Anisotropy in the direction of sediment transport (southwest–northeast), and rapid vertical variation to account for variability between individual sandstone beds, were achieved through use of an elongate oriented variogram. The average porosity of the Bunter Sandstone in the model is 15 %, while the average porosity of the non-cemented sandstone lithofacies is 18 %. As very few permeability data exist within the model area, permeability was assigned to the model using bivariate SGS, using the porosity distribution to guide the permeability values assigned to the grid. The correlation between porosity and permeability is provided by cross-plots of available core-plug data from across the Bunter Sandstone Formation. The arithmetic average permeability of the non-cemented sandstones in the model is 248 mD, while the geometric mean is 30 mD.

Porosity and permeability of the shale lithofacies, including the caprock shales, were assigned as 3 % and 6.5 x 10^{-3} mD respectively. These are rounded averages of those given by [7] for top sealing shales overlying the Bunter Sandstone in the Dutch Sector. In the base-case simulation, the cemented sandstones were given a very low porosity of 1 x 10^{-5}, and permeability of 6.5 x 10^{-3} mD. The distribution of porosity and permeability within the model are key uncertainties, and are therefore varied in the sensitivity analysis. Additional parameters required for reservoir simulation are largely taken from the UK SAP database [8].

4. Base-case reservoir simulation

A base-case dynamic simulation of CO_2 injection into Dome A was performed using ECLIPSE 300 with the CO2STORE module [9], in order to calculate the storage efficiency of the dome (E_d) using the equation below.

E_d = Volume of stored CO_2 (at reservoir conditions) / Total pore volume of dome

The total pore volume of each dome was calculated from the geocellular model by determining the pore volume above their respective spill-points, the total pore volume of Dome A being 12 km^3. As no relative permeability or capillary pressure measurements for CO_2/brine were available for the Bunter Sandstone, measurements from Bennion and Bachu's Viking 2 curves were used for sandstone, and Calmar values taken for the shale lithofacies [10 and 11].

4.1. Injection scenario

The aim of the reservoir simulation was to establish the storage efficiency and the factors that affect it. Availability of up to 20 Mt of CO_2 per annum, over an operational span of 50 years was therefore considered for storage. In order to inject as much of this CO_2 as possible, ten vertical injection wells were positioned in a circular configuration around the crest of each dome, along a constant depth contour, with perforations within every non-cemented sandstone layer. The objective here was to determine a range of achievable storage efficiency values rather than to establish an operational rationale for CO_2 injection projects. Initial modeling investigated the optimal distance of the wells from the crest of the dome, from which it was decided to place them so that the uppermost well completions were at a depth of 1300 m,

somewhat deeper than the crest of Dome A which lies at 1186 m, yet a reasonable distance from the shallowest spill-point depth (1730 m). Locating the injection wells at greater depths increases the likelihood that CO_2 will migrate from the dome via this spill-point. The initial injection rate for each well was 2 Mt/year/well, but injection was limited by pressure, and by CO_2 migration from the spill-points. An allowable bottom-hole pressure (BHP) limit of 90 % of the fracture pressure for that depth was stipulated, and the injection rates of individual wells were reduced in order to maintain the pressure below this threshold. In addition, a monitoring well was placed at the crest of each dome, and the simulation configured so that the injection rate in all wells was reduced by 20 % if the BHP exceeded 90 % of its fracture pressure.

Migration of CO_2 from the designated storage complex, defined by the limit of structural closure of the domes into which injection is taking place, was also monitored and used to limit the injection rate. A conservative level of leakage, 0.01 % of the injected CO_2 by mass (in both free and dissolved forms), was selected as the spillage criterion by which injection would be limited. If this limit was reached, then injection was ceased. If not, then injection would continue for a period of 50 years within the limitations of the BHPs.

4.2. Base-case simulation results

In the base-case simulation, pressure built up rapidly in some wells, and the injection rate was reduced accordingly. After 20 years of injection the spillage criterion was reached and injection ceased, resulting in an E_d of around 19 %, which corresponds to a CO_2 storage capacity of 331 Mt (mass of CO_2 injected). Therefore, in the base-case simulation, the limiting factors affecting CO_2 storage are a combination of both pressure build-up and CO_2 migration.

5. Sensitivity analysis

Due to the inherent uncertainty regarding some features of the model, sensitivity studies investigated the effect of varying the aquifer size and degree of heterogeneity. A further study investigated the effect of injecting CO_2 into adjacent domes, on the storage efficiency of Dome A.

5.1. Aquifer size

Although numerical aquifer volumes were used to represent the connected aquifer surrounding the geocellular model, it is uncertain as to whether the Bunter Sandstone may in fact be compartmentalized by unidentified faults and fracture zones, salt diapirism or igneous dykes. In order to address this uncertainty, a number of simulation cases were performed with varying aquifer volumes. The results of these in relation to the base-case are shown in Figure 3, and are described below:

- Geocellular model boundaries closed, with aquifer pore volume of 40 km^3.
- Dome A boundary closed, with aquifer pore volume of 12 km^3.
- Aquifer pore volume of 24,293 km^3 (effectively open model). This case assumes that displaced brine may be expelled via a seabed outcrop, as described by [3], providing a means of aquifer pressure relief.

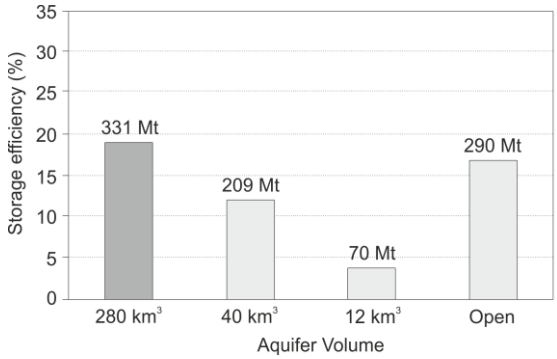

Fig. 3. Effect of varying connected aquifer volume on CO_2 storage efficiency. The achieved storage capacities are noted above the bins, and the base-case simulation results are shown in a darker shade of grey.

Unsurprisingly, the results show that the storage efficiency decreases as the size of the aquifer is reduced due to pressure build-up (displaced brine was unable to diffuse effectively throughout the aquifer). However, counter-intuitively the E_d in the open aquifer case was less than in the base-case. This is due to effective pressure diffusion through the aquifer meaning that under the prescribed injection scenario, the injection rate was able to be maintained, facilitating a more rapid migration of CO_2 towards the structural spill-point. This emphasizes the importance of different forces affecting the CO_2 plume, as in this case the maintained injection pressures force the CO_2 towards the edge of the defined storage complex.

5.2. Heterogeneity

Several simulation cases were performed to address the uncertainty regarding the reservoir properties. The results of these are shown in Figure 4a compared with the base-case simulation, and include:

- Removal of the laterally extensive cemented sandstone layer at the top of reservoir Zone 4.
- Decreasing the permeability of the cemented sandstone and shale lithofacies to zero (“Low K” on Figure 4a).
- Increasing the porosity and permeability of the cemented sandstone and shale lithofacies to 5 % and 1 mD respectively (“High K” on Figure 4a).
- Decreasing the ratio of vertical to horizontal permeability (Kv/Kh) to 0.1. (In the base case, Kv/Kh = 1.)
- Homogenous reservoir case with porosity of 15 % and permeability of 100 mD.

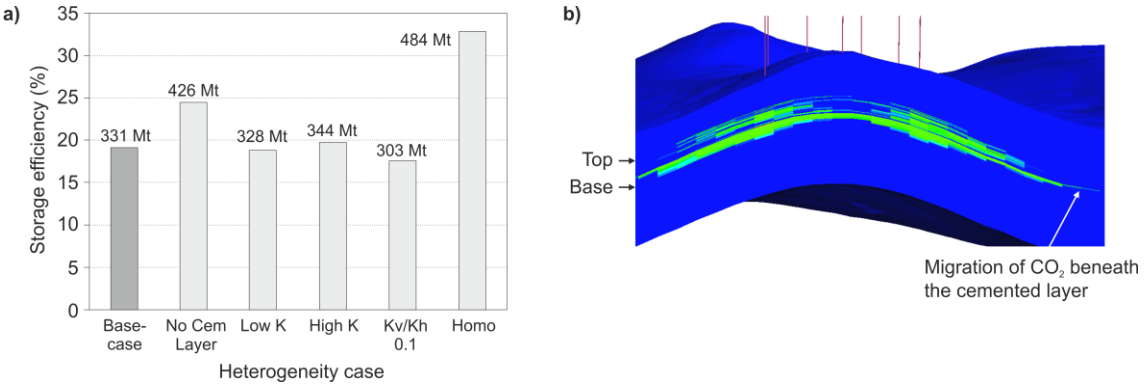

Fig. 4. a) Effect of varying the porosity and permeability of the Bunter Sandstone. Achieved storage capacities are shown above the bins. b) Cross-section through Dome A (view towards the northwest) showing the distribution of CO_2 in the base-case simulation (green) after 20 years of injection. The top and base of the Bunter Sandstone are shown on the left-hand side. Note that the CO_2 migrates beneath the cemented layer towards the spill-point (into Dome B).

Removal of the continuous cemented layer has a marked effect on the storage efficiency of the dome, because its presence in the base-case simulation prevents the CO_2 in the lower part of the reservoir from rising buoyantly to the crest of the dome where it is more likely to become structurally trapped (Figure 4b). Thus, less of the CO_2 migrates beneath this layer towards the structural spill-point, as it does in the base-case simulation. Figure 4a shows that both increasing, and decreasing the porosity and permeability of the cemented sandstone and shale lithofacies, has a relatively minor effect on the storage efficiency while decreasing the ratio of vertical to horizontal permeability results in a clear decrease in E_d. The homogenous reservoir case yields the highest storage efficiency, with CO_2 rising unimpeded to the crest of the dome where it becomes trapped within the structure.

6. Conclusions

The results presented here show that the potential storage efficiencies are linked to the size of the connected aquifer, the reservoir heterogeneity, and to the injection strategy. With the exception of the closed model cases, all of the simulations were limited by CO_2 migration from the dome via spill-points, although the injection rate in every case was reduced in order to avoid reaching the fracture pressure. The simulations indicate that the E_d, and thus the storage capacity, is governed by a complex interaction between geological structure and reservoir heterogeneity, necessitating accurate characterization within reservoir models for studies of CO_2 storage. Accurate delineation of the structure and its potential spill-points is required if a spillage criterion is introduced as a constraint on injection. The simulations also suggest that a delicate balance exists between the viscous and gravity forces acting on the CO_2, which may be managed through careful monitoring and control of the injection wells.

Another factor which will affect the storage efficiency is the extent of the boundary at which it is considered acceptable for CO_2 to contact. In the simulation cases described here, 0.01 % of the CO_2 by mass leaving the shallowest spill-point of Dome A was considered to be the threshold at which injection would cease. However, Domes A and B share a common spill-point (Figure 1). Therefore, if injection of CO_2 is initiated simultaneously into Domes A, B and C, the storage efficiency of Dome A increases to 28

% if CO_2 is permitted to migrate freely between them. The pore volume-weighted average storage efficiency across the three structures was 18 %, similar, but slightly lower than the storage efficiency of Dome A in the base-case simulation. It is expected that the storage efficiency will decrease when injecting into multiple domes due to pressure build-up. It should be noted, that the storage efficiencies given here are calculated according to the pore volume of the domes, and not that of the entire connected aquifer volume. The total aquifer storage efficiency varies from 0.1 to 0.8 % across the simulation cases described here.

Acknowledgements

This study was commissioned and funded by the UK Energy Technologies Institute as part of the UK Storage Appraisal Project. We thank the Energy Technologies Institute for permission to publish this work. The BGS authors publish with the permission of the Executive Director, British Geological Survey (NERC). The Heriot-Watt authors thank Schlumberger for the use of ECLIPSE.

References

[1] Holloway S, Vincent CJ, Bentham MS, Kirk KL. Top-down and bottom-up estimates of CO_2 storage capacity in the UK sector of the Southern North Sea Basin. *Environmental Geoscience.* 2006; **13**: 74–81.

[2] Smith DJ, Noy DJ, Holloway S, Chadwick RA. The impact of boundary conditions on CO_2 storage capacity estimation. *Energy Procedia*. 2010; **4**: 4828–4834.

[3] Noy DJ, Holloway S, Chadwick RA, Williams JDO, Hannis SA, Lahann RW. Modelling large-scale carbon dioxide injection into the Bunter Sandstone in the UK Southern North Sea. *IJGGC*. 2012; **9**: 220–233.

[4] Bifani R. Esmond Gas Complex. In: Brooks J, Goff JC, Van Hoorn B, editors. *Habitat of Palaeozoic Gas in N.W. Europe,* London: Geological Society Special Publications, 1986; **23**: 209–221.

[5] Ritchie JS, Pratsides P. The Caister fields, Block 44/23a, UK North Sea. In: Parker JR, editor. *Petroleum Geology of Northwest Europe: Proceedings of the Fourth Conference*. London: Geological Society, 1993; 759–769.

[6] Cameron TDJ, Crosby A, Balson PS, Jeffery DH, Lott GK, Bulat J, Harrison DJ. *The Geology of the Southern North Sea*. London: British Geological Survey and HMSO; 2006.

[7] Spain DR, Conrad CP. Quantitative analysis of top-seal capacity: Offshore Netherlands, Southern North Sea. *Geologie en Mijnbouw*. 1997; **76**: 217–226.

[8] Gammer D, Green A, Holloway S, Smith G. The Energy Technologies Institute's UK CO_2 Storage Appraisal Project (UKSAP). *SPE paper 148426*, presented at the SPE Offshore Europe Oil and Gas Conference, Aberdeen. 2011.

[9] Schlumberger. Eclipse 300 Technical Manual. 2010.

[10] Bennion DB, Bachu S. The impact of interfacial tension and pore-size distribution/capillary pressure character on CO_2 relative permeability at reservoir conditions in CO_2-brine systems. *SPE paper 99326*, presented at the SPE/DOE Symposium on Improved Oil Recovery, Tulsa. 2006.

[11] Bennion DB, Bachu S. Drainage and imbibition relative permeability relationships for supercritical CO_2/brine and H_2S/brine systems in intergranular sandstone, carbonate, shale and anhydrite rocks. *SPE paper 99326*, *SPE Reservoir Evaluation and Engineering*, 2008; **11**: 487–496.